ADVANCED FUNCTIONAL MATERIALS
www.afm-journal.de

Extraordinarily Sensitive and Low-Voltage Operational Cloth-Based Electronic Skin for Wearable Sensing and Multifunctional Integration Uses: A Tactile-Induced Insulating-to-Conducting Transition

*Ying-Chih Lai, Bo-Wei Ye, Chun-Fu Lu, Chien-Tung Chen, Meng-Huan Jao, Wei-Fang Su, Wen-Yi Hung, Tai-Yuan Lin, and Yang-Fang Chen**

Electronic skin sensing devices are an emerging technology and have substantial demand in vast practical fields including wearable sensing, robotics, and user-interactive interfaces. In order to imitate or even outperform the capabilities of natural skin, the keen exploration of materials, device structures, and new functions is desired. However, the very high resistance and the inadequate current switching and sensitivity of reported electronic skins hinder to further develop and explore the promising uses of the emerging sensing devices. Here, a novel resistive cloth-based skin-like sensor device is reported that possesses unprecedented features including ultrahigh current-switching behavior of ≈10^7 and giant high sensitivity of 1.04×10^4–6.57×10^6 kPa^{-1} in a low-pressure region of <3 kPa. Notably, both superior features can be achieved by a very low working voltage of 0.1 V. Taking these remarkable traits, the device not only exhibits excellent sensing abilities to various mechanical forces, meeting various applications required for skin-like sensors, but also demonstrates a unique competence to facile integration with other functional devices for various purposes with ultrasensitive capabilities. Therefore, the new methodologies presented here enable to greatly enlarge and advance the development of versatile electronic skin applications.

Dr. Y.-C. Lai, C.-T. Chen, Prof. Y.-F. Chen
Department of Physics
National Taiwan University
Taipei 106, Taiwan
E-mail: yfchen@phys.ntu.edu.tw
B.-W. Ye
Graduate Institute of Applied Physics
National Taiwan University
Taipei 106, Taiwan
C.-F. Lu, M.-H. Jao, Prof. W.-F. Su
Department of Materials Science and Engineering
National Taiwan University
Taipei 106, Taiwan
Prof. W.-Y. Hung, Prof. T.-Y. Lin
Institute of Optoelectronics Sciences
National Taiwan Ocean University
Keelung City 202, Taiwan
Prof. Y.-F. Chen
Center for Emerging Material and Advanced Devices
National Taiwan University
Taipei 106, Taiwan

DOI: 10.1002/adfm.201503606

1. Introduction

Human skin can sense touch, strain, and vibration and provide important information of surroundings for human, therefore human can "feel" and respond with appropriate action. According to the capability of natural skin, developing highly sensitive, flexible, wearable, and even capable of self-healing "skin-like" sensors, i.e., electronic skin (e-skin), in artificial systems is an emerging technology and potentially has substantial demand in various practical fields.[1–7] For example, mimicking the tactility of skin in electronic systems can offer seamless human–computer interactive interfaces for intuitive and instantaneous feedback, showing promising applications including touch-driven or gesture-control interfaces with digital electronics and smart objects.[8–11] Additionally, flexible sensors recreating skin's sensibility can employ in sensing or mapping touch of biomimetic prosthesis and robots' skins.[12–14] Moreover, developing wearable "skin-like" sensors on clothing, beds, or directly wrapped around body can widely avail in real-time monitoring human motion or physiological signals, opening new opportunities for anytime anywhere healthcare applications.[15–20] However, to date, single e-skin that can simultaneously possess high sensitivity and be able to integrate with other electronic devices for advanced functions in low-pressure regime (<1 kPa) has not been realized yet.

Several technologies have been proposed for developing "skin-like" pressure sensors, including capacitive, piezoresistive, piezoelectric, and triboelectric methodologies.[3,17,21–23] Among various technologies, resistive "skin-like" sensors have been considered as a favorable technology for e-skin applications due to their advantages of superior sensitivity, simple read-out mechanism, simplicity in device design, and cost-effective fabrication.[13–17] In particular, they promise a remarkable potential for direct integration with other functional electronic components, simultaneously acting mechanical sensors and seamless user-interactive interfaces.[7,8,11] This merit can

largely simplify the design of user-interaction systems perceiving directly through the sensing and open opportunities for further devising multipurpose e-skin uses without complicated computing circuits and electronic boards, thus fairly benefiting the development of wearable/disposable e-skin systems that are highly required to be simple, lightweight, and even imperceptible.[7,8,17,24] Most efforts have been focused on investigating new materials for higher sensitivity at low-pressure regime (<10 kPa) and building low-cost and scalable manufacturing strategies.[13–18] Although highly sensitive e-skins have been achieved, great obstacles still exist when considering them as smart interactive devices and further integrating the sensing capabilities with other devices for multifunctional applications. This hurdle arises from the insufficient pressure-introduced current switching and the fact that the pressure-responsive (turn-on) current of resistive e-skins remains quite low.[11,13–18] Although Wang et al. reported user-interactive e-skins for pressure visualization by integrating pressure sensors with organic light-emitting diodes (OLEDs), visible signals can only be obtained by applied pressures less than ≈10 kPa with a large voltage of 10 V.[8] Tee et al. demonstrated a self-healing e-skin to drive a light-emitting diode (LED) with pressures > ≈50 kPa.[7] Most recently, Chou et al. reported a chameleon-inspired e-skin; however, the reaction needed pressures large than 10 kPa and the integration required an external amplifier circuit.[11] Despite of the promising demonstrations, the need of fairly large pressures and driven voltages is a great drawback. Furthermore, the inadequate sensitivity makes the computing systems hard to readily distinguish the on/off signals, limiting the utilization of ultrasensitive e-skins in embedded systems for more sophisticated applications.

Moreover, progress in resistive e-skin only involves exploring the devices by using plastic or elastic substrates, such as poly(ethylene terephthalate) and poly(dimethylsiloxane) (PDMS),[11,13–18] limiting the promising utilization of e-skins. In terms of wearable electronics, flexible and stretchable cloths can offer alternative substrates that are hygroscopic, genial, and more breathable and comfortable than airtight polymers or plastic substrates.[25] Particularly, devising e-skin sensors based on cloth can facilely join textile articles, such as garments or beds, greatly broadening their applications in cloth-based uses.[25–27] However, till now, there is no report using cloth for designing resistive e-skins.

Here, we present a new type of cloth-based resistive e-skin with unprecedented features including ultrahigh current-switching ratios of $\approx 10^7$ orders and an ultrahigh sensitivity of 1.04×10^4–6.57×10^6 kPa^{-1} in a low-pressure regime of <3 kPa. And, notably, both features were achieved by a low working voltage of 0.1 V. Taking these remarkable traits, our device not only functions as an ultrasensitive e-skin sensor but also, for the first time, enables to directly incorporate with other functional devices, such as solar cells or other optoelectronic components, for versatile integrated uses with the unique sensing capabilities in low-pressure regime. The newly-designed e-skin was fabricated based on a cloth substrate and constructed by two stainless-steel threads as bottom electrodes and a suspended silver nanowires-surface-embedded PDMS (AgNW/PDMS) as conducting film. Appling a pressure onto the device will induce the contact spots between the suspended AgNW network and the two bottom conductive threads, resulting in an abrupt transconductance and a pressure-sensitive current flow between the two bottom electrodes at a fixed bias. Beyond considerable switching behavior and superior sensitivity, our device also features comparable fast response/relaxation time (4/16 ms), low detection limit (0.6 Pa), and high stability (>5000 cycles). In addition, the capability of identifying different mechanical forces, including touching, bending, twisting, and stretching forces, has been demonstrated. With the cloth substrates, our devices can be facilely attached to collar and wristband for sound recognition and detection hand motions, respectively. In particular, based on its exceptional features, the first demonstration of fully autonomous indoor-light-powered e-skin system has been successfully performed for information transmission by integration with a photovoltaic cell, which can greatly advance the development of self-green-powered e-skin systems, such as disposable sensing wristband and indoor-light-powered robotics' skins. Moreover, for the first time, by integrating our device with optoelectronic components, visually human-readable e-skin can be realized in a low-pressure regime <1 kPa without supplementary circuits. Furthermore, as a proof-of-concept for more sophisticated applications, our device can function as a wireless sound controller and wireless medical-bed monitor by incorporating with signal processing units. These remarkable features and advantages have not been achieved in previous reports, which enable to greatly broaden and advance the applications of e-skins. The presented work is based on low-temperature and cost-effective fabrication processes and facilities, promising for industrial-friendly manufacturing.

2. Results

2.1. Device Structure and Working Principle

Figure 1a illustrates the schematic fabrication processes. We chose AgNWs as conducting film due to their excellent conductivity, flexibility, stretchability, and low-cost manufacturability advantages.[28] Fabrication details are presented in Supporting Information Section 1. Briefly, a patterned well-welded AgNW network was embedded on the surface of PDMS film. After washing, the border of as-prepared PDMS was glued onto the cloth substrate that was prestitched with two isolated conductive threads as bottom electrodes. Following by curing to stick the PDMS border onto the cloth substrate, the central conducting AgNW/PDMS film was spontaneously bulged upward and suspended above the two conductive threads. This bulged central part of PDMS was attributed to the swell of PDMS and the mezzanine air between PDMS and the cloth substrate during thermal curing. Note that because the border of PDMS was fixed on the cloth, the thermal expansion of PDMS and the mezzanine air led the central part of PDMS to bulge. Figure 1b and Figure S1 (Supporting Information) show the resulted e-skin with the demonstration of its flexibility and stretchability. The bulged PDMS with air gap between the AgNW/PDMS and conductive threads can be clearly observed in Figure 1c and Figure S2 (Supporting Information). The AgNW networks were well-welded and sturdily embedded onto the PDMS surface, as shown in the scanning electron microscopy (SEM) images of

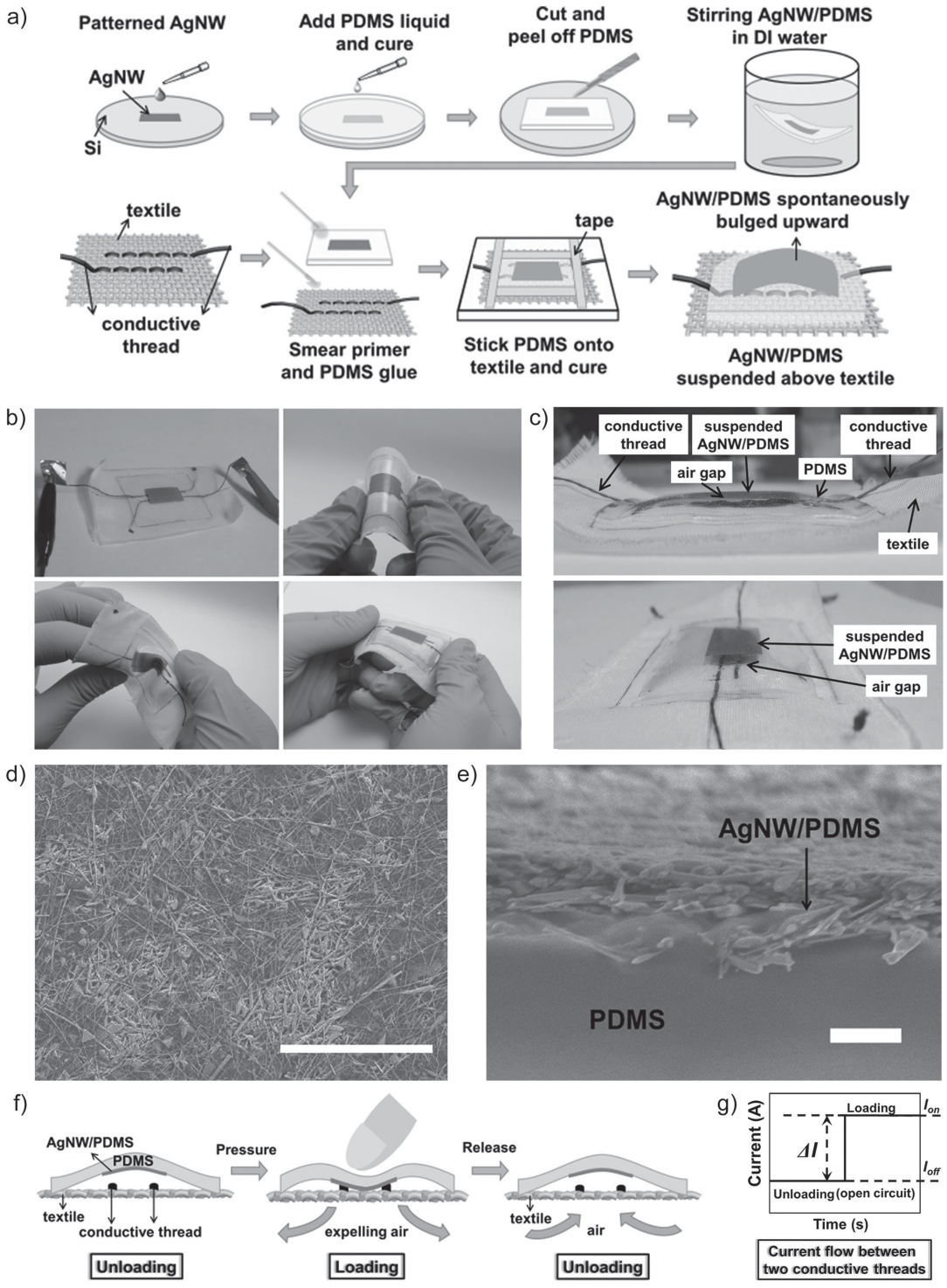

Figure 1. a) Schematic diagram for the fabrication process of the cloth-based e-skin. b) Photographs of as-prepared e-skin with demonstrations of its flexibility and stretchability. c) Front-view (top) and side-view (bottom) photographs of as-prepared e-skin. d) Top-view SEM image of the AgNW/PDMS. e) Side-view SEM image of AgNW/PDMS. f) Schematic illustration of the sensing mechanism. g) Schematic illustration of the current changes in responses of loading and unloading (I_{off} (open circuit): unloading; I_{on}: loading).

AgNW/PDMS (Figure 1d,e and Figure S3, Supporting Information). The resulted AgNW/PDMS showed a sheet resistance of ≈2.08 Ω sq^{-1} from the four-point probe measurement, indicative of the high conductivity of the AgNW network. Figure S4 (Supporting Information) shows the SEM image of the cloth substrate with numerous vents between the fabrics. Figure S5 (Supporting Information) shows SEM image of the conductive thread which was spun from many stainless-steel fibers.

The working principles of the cloth-based e-skin are mainly through the contact resistance mechanisms, which are schematically illustrated in Figure 1f,g. In the beginning, a fixed bias was applied on the two isolated conductive threads, and the AgNW/PDMS was initially suspended above the textile, leading to the two conductive threads at a break state when no force was applied on the device. Applying an external force can easily extrude the mezzanine air from the textile and make the contacts between bottom electrodes and AgNW/PDMS. And, the detected current flow between the two electrodes arises from the force-dependent discrete contact spots among the asperities of AgNW/PDMS film and the two conductive threads. The effective AgNW bridges between the two conducting threads depend on the external forces applied. It is worth noting that both conducting AgNW/PDMS film and conductive threads have very rough surfaces, making the contact resistance very sensitive to applied pressures. After releasing the applied force, the AgNW/PDMS can easily recover to the initial bulged state.

2.2. Pressure Sensing Measurements

To explore the pressure responses of the presented e-skin tactile sensor, we applied bias between two conductive threads and measured the current flow upon different applied pressures on the device. **Figure 2**a depicts the pressure responses of our device. The linear relationship of the *I*–*V* curves indicates that the device conforms to Ohmic resistance after applying pressures and the current levels reveal obvious increase as external pressures increase. With no pressure applied, the conducting AgNW/PDMS does not contact with the bottom conductive threads, making the OFF-state initially at a break status. Figure 2b shows the statistic results of the current levels and I_{on}/I_{off} switching ratios as a function of applied pressures under a fixed operating voltage of 0.1 V. (I_{off} denotes the initial current with no applied pressure; I_{on} denotes the current under applied pressures.) The current flow shows a sharp switching behavior with considerable I_{on}/I_{off} ratio of $\approx 10^7$ when applied pressure increases from 0 to ≈1 kPa. To our knowledge, the switching ratio of $\approx 10^7$ orders at the low-pressure regime of <1 kPa is the highest value reported so far and much higher than all pressure-induced switching ratios reported recently (Table S1, Supporting Information),[11–20] for example, the pressure sensors fabricated based on microstructured conducting polymer ($\approx 10^3$ at 1 kPa),[13] and CNT/PDMS composite ($\approx 10^4$ at 1 kPa).[17] The extreme current-switching behavior can be attributed to the fact that the OFF-state is initially at a break insulating condition; when applying pressures, a high ON-state current flow can be attained by the well-welded highly conducting AgNW/PDMS film that bridges the two conductive threads. The considerable on/off feature can provide readily distinguished signals in response to different applied pressures, which is quite favorable for e-skins acting as user-interactive switches based on their unique ultrasensitive capability.[29–31] The statistics of the current switching from five difference devices are presented in Figure S6 (Supporting Information). The small variation indicates that our new device can serve as an excellent pressure switch and sensor.

It is worth noting that the great I_{on}/I_{off} ratio is achieved only by a very low driving voltage of 0.1 V, which can be ascribed to the highly conducting pathways supplied by the AgNW bridges. Compared with all published literatures, this working voltage of 0.1 V with such high switching ratios is the lowest reported value (Table S1, Supporting Information).[11–20] For example, it is much lower than previous works of CNT/PDMS e-skins (10 V)[17] and suspended-gate pressure-sensitive transistor (60 V).[20] The low operating voltage suggests that our e-skin device can be simply driven by a portable battery, or green power sources, such as flexible solar cells[32] or triboelectric generators,[33] showing its potential of practical applications.

In addition to exceptional switching behavior, our device also exhibits an unprecedented sensitivity, as shown in Figure 2c. Here, the pressure sensitivity is defined as $S = (\Delta I/I_{off})/\Delta P$.[13] ($\Delta I$ denotes the current change upon applied pressure and ΔP denotes the applied pressure.) We analyzed by current platform because the current-sensing capabilities are much more important in developing multifunctional e-skin applications.[17] As depicted in Figure 2c, the device reveals an extremely-high sensitivity of $\approx 1.04 \times 10^4$–9.30×10^5 kPa^{-1} within a pressure regime of <100 Pa. Over the pressure range from 380 Pa to 3 kPa, the device shows a sensitivity of $\approx 2.72 \times 10^6$–6.57×10^6 kPa^{-1}. This value sets a new record of sensitivity in low-pressure region among previous reported flexible pressure sensors (Table S1, Supporting Information)[11–20] and is higher than previous records of pressure sensors based on suspended-gate transistors (192 kPa^{-1}, <5 kPa),[20] and microstructured conducting polymer (≈0.2–133.1 kPa^{-1}, <3 kPa).[13] The extraordinary sensitivity can mainly be attributed to two reasons: (i) the ultrahigh switching of current flow and (ii) very large force-dependent contact spots between AgNW/PDMS and two bottom electrodes. The former is achieved by the transition from the initial break of OFF-state transforming to the highly conducting ON-state caused by the well-welded AgNWs bridging the two conductive threads. And, the latter arises from the rough contact surface that does not only come from the top AgNW/PDMS film but also from the multistrand-twisted conductive fibers of two bottom electrodes, which endows a large number of force-dependent contact spots. Indeed, previous works have reported that rough electrodes can effectively promote the sensitivity of pressure sensors.[13] A real-time monitoring output current under different pressures has been performed in Figure S7 (Supporting Information), indicating the stable and distinct I_{on}/I_{off} in response to different applied pressures of our devices.

Moreover, our device displays instantaneous responses to both external loading and unloading with favorable response and relaxation time of ≈4 ms and ≈16 ms (Figure 2d), respectively, which is better than most previous results.[11–20] The device also exhibits excellent reliability based on the fact that after loading/unloading a pressure of 500 Pa for 5000 cycles it still shows manifestly distinguished response to the loading with a similar switching ratio (Figure 2e). To investigate the detection limitation,[13,15] we placed a small flower (≈12 mg) onto the e-skin device covered with a tuned glass slide (2 cm × 1 cm, 0.5 g) and measured the real-time *I*–*t* response upon placement/removal of the small flower (Figure 2f). Our device demonstrates ready recognition to the tiny loading of flower (corresponding to ≈0.6 Pa)

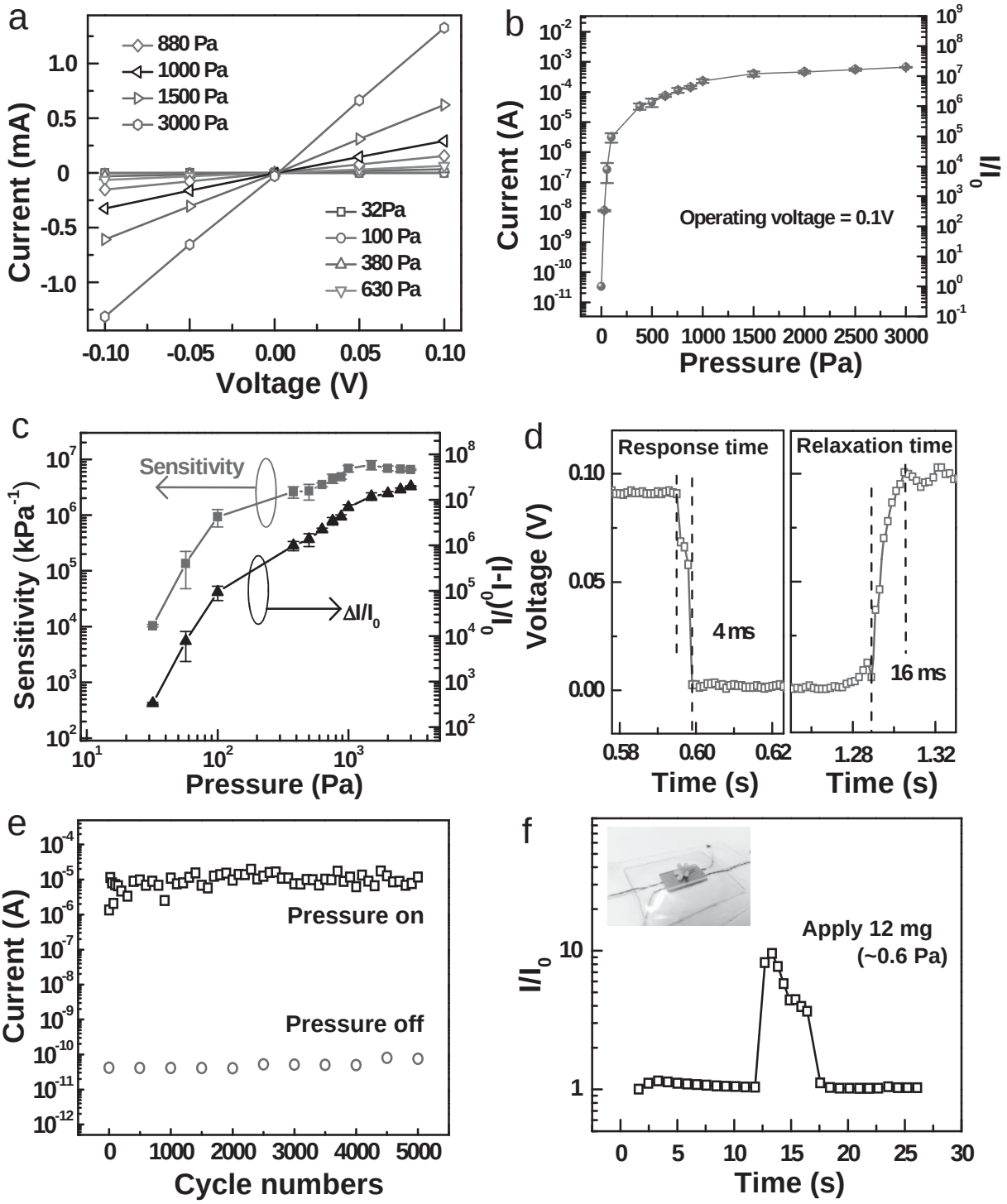

Figure 2. a) *I–V* curves of the device with applied different pressures. b) Static results of the current response and on/off current ratio under various pressures at 0.1 V. c) Pressure sensitivity and current changes under various pressures. The error bars represent one standard deviation. d) Response (left)/release (right) time of the device with loading/unloading a pressure of 2.5 kPa. e) Current of the device under loading/unloading a pressure of 500 Pa over 5000 cycles. f) Real-time response to the application/removal of a flower with a minute weight of 12 mg corresponding to 0.6 Pa on the device.

with an outstanding sensitivity of ≈7.77 × 10^3 kPa^{-1}, indicative of its sensing capability in subtle forces with an obvious sensitivity. In contrast to previous reports,[11–20] our device not only shows comparable low detection limit but also offers significantly higher sensitivity to subtle pressures. These outstanding features confirm that our newly-designed sensing device can meet various kinds of applications where skin-like tactile sensing is desired.

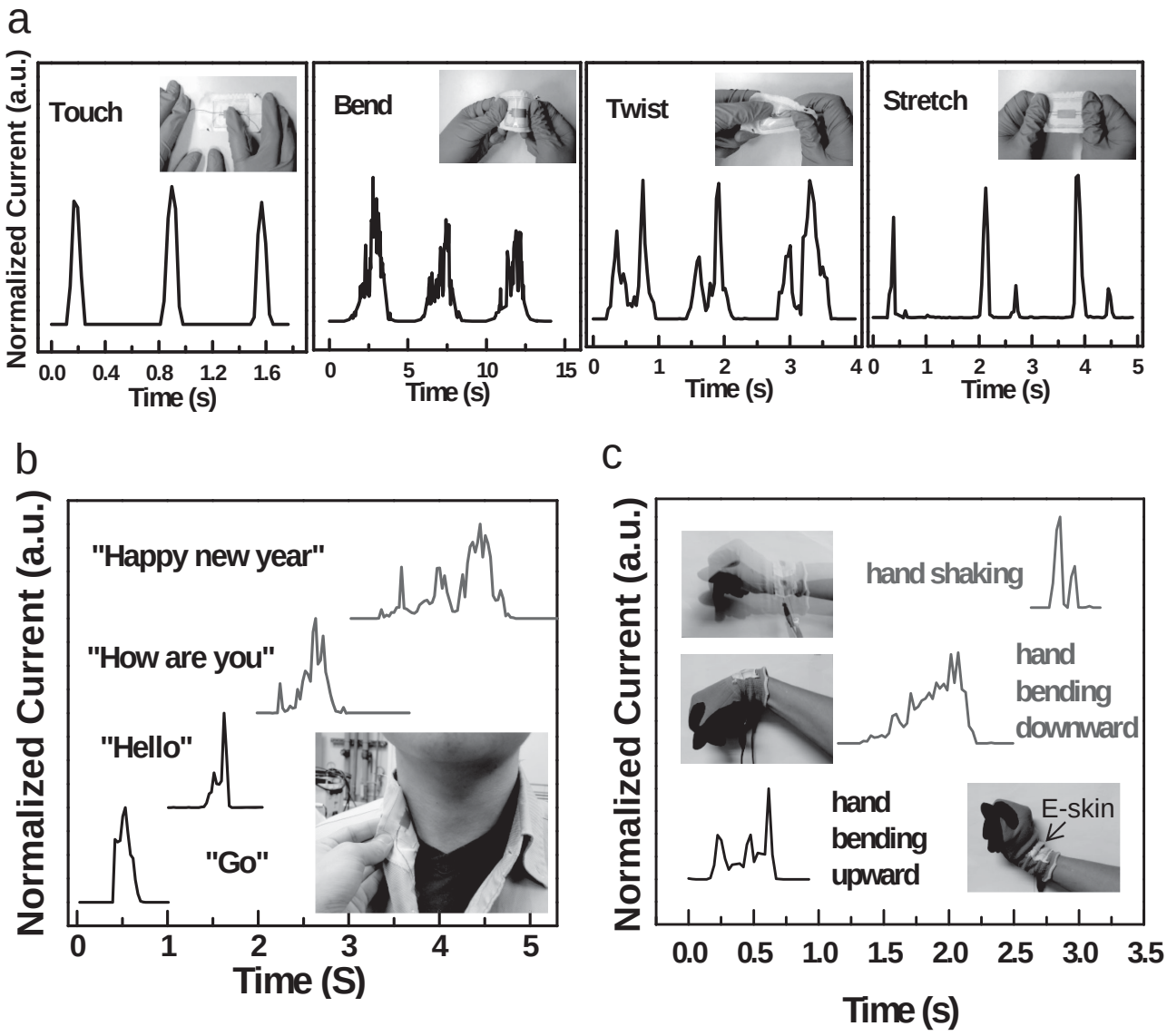

Figure 3. a) Real-time current responses to different mechanical forces including touching, bending, twisting, and stretching forces. b) Real-time current responses to different sentences spoken by the tester. The inset shows the photographs of as-prepared device attached onto the collar of shirt worn on the tester. c) Real-time current responses to different hand motion.

2.3. Detection of Various Mechanical Forces and Wearable Sensing Applications

In addition to pressure sensing, our device also revealed good recognition capabilities to different mechanical forcing, including touch, bend, twist, and stretch, with excellent signal-to-noise ratios, as shown in the real-time detection of various mechanical forces (**Figure 3**a). These results suggest its promising applications in monitoring various mechanical deformation and muscle motions. Together with the merits of cloth substrate, our e-skin device can facilely merge into textile-based wearable articles, such as garment, gloves, or wristbands, for diverse monitoring purposes. For example, we mounted our device onto the shirt collar and tested it for sensing throat motions during different sentences spoken. As shown in Figure 3b, our sensor exhibited excellent voice recognition to different spoken phrases with good reproducibility (Figure S8, Supporting Information), implying its potential uses in wearable voice controllers, concealed microphones, and conformable electronic throats for collecting and reproducing voice of patients who have voice troubles.[15] Furthermore, stitching our cloth-based e-skin device onto the wristband of glove can be used for monitoring various hand motions, as shown in Figure 3c and Figure S9 (Supporting Information). These results suggest the potential capability of our skin-like sensors applied in wearable gesture controller and various healthcare and medical fields. For instance, utilizing in the cloth of Parkinson's patients may sense hands tremor and further control medicine release,[34] and mounting on sleeve opening or wristband of clothing may be used for assessing walking steps or sleeping quality.

2.4. Multifunctional Integrations

Beyond superior sensing capabilities, our device possessed the exceptional advantages of very low driving voltage of 0.1 V with extremely-high current switching in the low-pressure region. This unique virtue allows us to easily integrate e-skins with other devices for multifunctional uses with their sensing capabilities and without the need of additional computing systems and complicated circuits, showing large merits for developing wearable/portable/disposable system-level e-skin that are highly desired to be small and lightweight. For example, in previous resistive e-skins, the shortcomings of high resistance, insufficient sensitivity, and high working voltage cause difficulties in integrating with independent/green/portable power sources.[4–6,11–20,24] Here, by using the outstanding features of our device, we demonstrate the first fully autonomous self-indoor-light-powered e-skin system as user-interactive transducer, as shown in **Figure 4**a. This prototype is constructed by connecting our e-skin sensor with a perovskite solar cell and a resistor in series, and an oscilloscope was used for monitoring the voltage change of the resistor during touching our e-skin.[14] Figure 4b shows the efficiency and open voltage of the perovskite solar cell under AM1.5 (100 mW cm^{-2}) and indoor-light (5 mW cm^{-2}) illumination. Note that in this system, there is no external power supply, and we operated this system directly under indoor light, in which the efficiency of the photovoltaic cell was only 0.32% instead of 10.00% under AM1.5 illumination. Despite the efficiency being quite low under indoor light, the open voltage can retain ≈0.79 V (Figure 4b). We then touched our e-skin sensor and monitored the bias change of the resistor. Remarkably, it is found that the system can function very well as information transmission under only indoor light illumination, and, notably, it is insensitive to the efficiency of photovoltaics (Multimedia 1, Supporting Information). In Figure 4c, we input Morse codes by touching our device, and the codes can be clearly observed from the oscilloscope corresponding to the characters "Y," "E," and "S." This demonstration shows, as the first example, that a fully-autonomous e-skin system can be directly driven by photovoltaic cells and, notably, can function even only under indoor light illumination with being less dependent on the photovoltaics' efficiency. From application perspective, the weak dependence on efficiency shows an exciting opportunity for system-level e-skins integrated with flexible photovoltaics and directly working in places with weak light illumination, which can greatly enlarge the applications of e-skin in various fields and advance the development of green and low-cost fully-autonomous e-skin modules, such as disposable sensing wristband, indoor-light-powered robotics' skins, and human-interactive interfaces.

Integrating e-skins with electroluminescent/electrochromic devices (ECDs) can make external mechanical forces become visible signals, imparting e-skins' responses not only electrical-readable but also human-readable.[8,11] Thus, we integrated our e-skin with an OLED (Figure 4d and Multimedia 2, Supporting Information). Figure S10 (Supporting Information) shows the electrical characteristic and spectrum of the OLED. Figure 4e exhibits the *I–V* characteristic of the configuration under different applied pressures. As shown in Figure 4e, starting from the applied pressures larger than 32 Pa, a drastic increase of current flow can be clearly observed, and the responsive current increases with increasing the applied pressures. Figure 4f summarizes the current and related brightness in response to applied pressures. Compared to previous reports based on the integration of pressure-sensitive rubber with OLED that visible signals (>1 Cd m^{-2}) can only be obtained by pressures below ≈10 kPa,[8] our e-skin shows significant improvement in visible responsive signals at low-pressure region <1 kPa, which is far below the limitation in previously reported devices. The sensitivities of the visible pressure-sensitive signals have been evaluated to have the values of 75.09–285.72 Cd m^{-2} kPa^{-1} at low-pressure regime <1 kPa (Figure S11, Supporting Information), which are superior to a previous report of 42.7 Cd m^{-2} kPa^{-1} at 10–100 kPa.[8] Figure S12 (Supporting Information) shows real-time electroluminescent intensity under different pressures, indicating that the electroluminescent intensity of the OLED can respond rapidly and be readily identified to different applied pressures. Also, the OLED can be fast recovered after releasing loadings without significant hysteresis.

In addition to OLED, we also demonstrated the integration of our e-skin with an ECD having a device area of 4 × 4 cm^2, as shown in Figure 4g with a schematic circuit diagram below. Similar to OLED, the ECD can offer visible responses to the applied sensors and, furthermore, the initial transparency of ECD endows them for the applications in different fields, such as smart windows, transparent displays, etc. Most recently, Chou et al. reported a chameleon-inspired e-skin, in which the integration can change color by touching e-skin device.[11] Integration of e-skin with an ECD can be used in a user-interactive smart window that changes from transparence to deep color. The fabrication processes of the ECD can be found in the Supporting Information and the transmittance spectra regarding the ECD are shown in Figure S13 (Supporting Information). In this design, we applied a bias of 3.6 V to the system and detected the transmittance change of the ECD at the wavelength of 605 nm during different applied pressures. As shown in Figure 4h, the transmittance of the ECD changes instantaneously as the different pressures are applied and can be visually observed, indicating that the appearance of the ECD changes from transparent to deep colored state by introducing the application of pressures. Also, the ECD can be fast recovered to its initial transmittance after releasing the pressure without significant hysteresis. The resulted pressure-sensitive transmittance is summarized in Figure S14 (Supporting Information) and the sensitivity of this design has been extracted to be 3.34–0.29 kPa^{-1} in the low-pressure region (<1 kPa). Compared with the recently-reported chameleon-inspired e-skin which changes color by requiring applied pressures larger than 10 kPa, our device shows rapider reaction without hysteresis and greater sensitivity in low-pressure region (≤10 kPa), which is more comparable with human gentle touches.[11] Moreover, in contrast with previous results that required an external amplifier circuit,[11] our device can be directly connected with functional devices, which can largely simplify the designs and benefit the fabrication of lightweight modules.

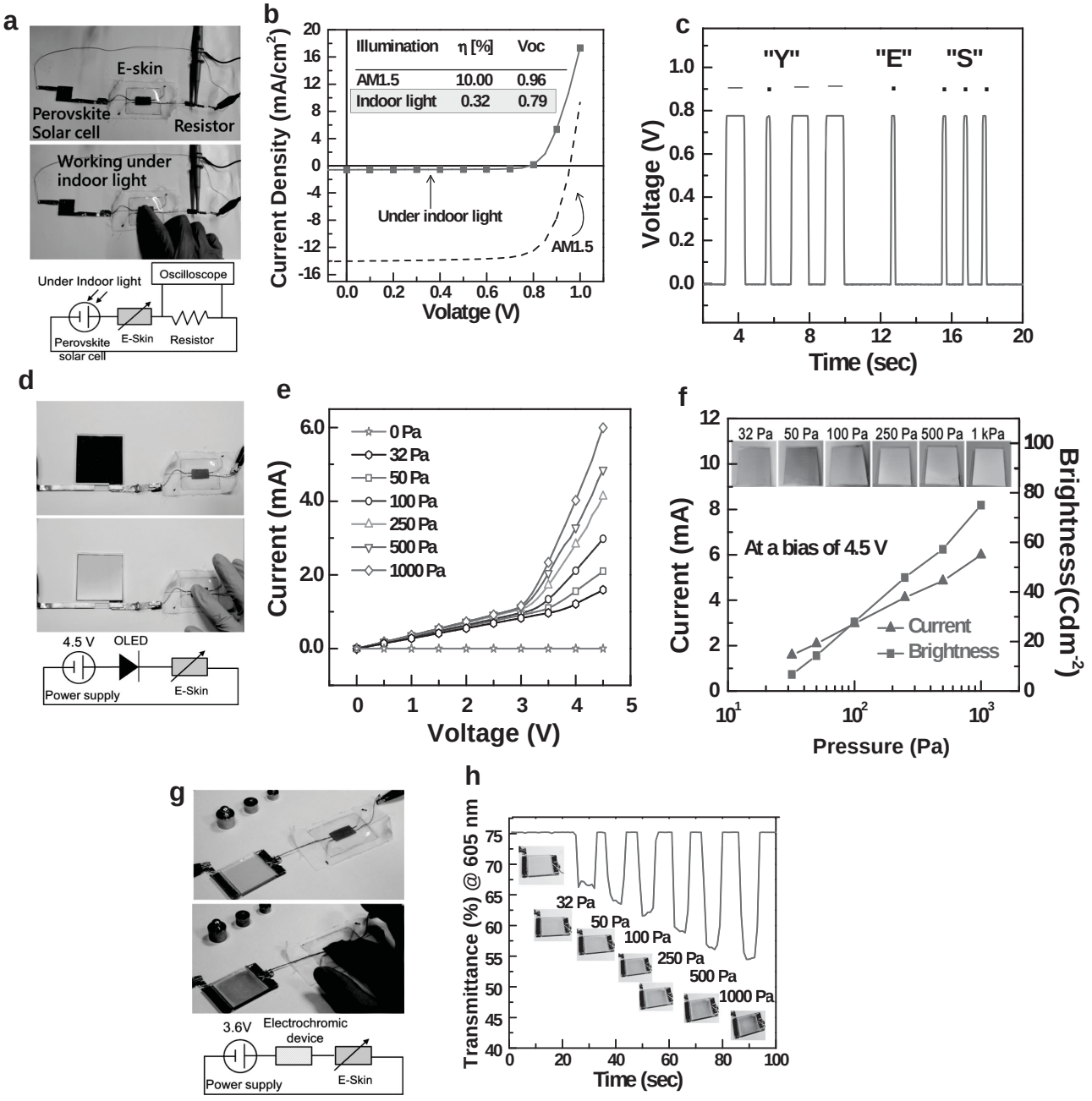

Figure 4. a) Photographs of as-prepared e-skin connected with a perovskite solar cell and 1 MΩ resistor, and oscilloscope was used to detect the potential difference of resistor. Schematic circuit of the transmitting information. b) *J–V* characteristics of the perovskite solar cell under AM1.5 and indoor-light illumination. c) Morse codes produced by touching the e-skin with finger, representing the characters "Y," "E," and "S." d) Photographs and circuit schematic (bottom) of the integration of as-prepared e-skin and OLED. e) *I–V* characteristics of the integration of as-prepared device and OLED under various applied pressures. f) The current and brightness of OLED as a function of applied pressure at a bias of 4.5 V. Inset: Photographs of the OLED in response to different applied pressures. g) Photographs and circuit schematic (bottom) of the integration of e-skin and ECD. h) Real-time response of transmittance of ECD at the wavelength of 605 nm under various applied pressures. The applied bias is affixed at 3.6 V. Inset: Photographs of the ECD in response to different applied pressures.

2.5. Human-System Interactive Applications

For more sophisticated usage, because our device possesses ultrahigh switching ratios, it enables to distinctly distinguish the sensing signals, rendering them fairly suitable for integration with working systems as smart interfaces for versatile applications that can give commands directly through the sensing.[29–31] **Figure 5**a(left) shows an example of using our e-skin sensing device as a wireless sound controller system, in which our device was integrated with a microcontroller with a wireless

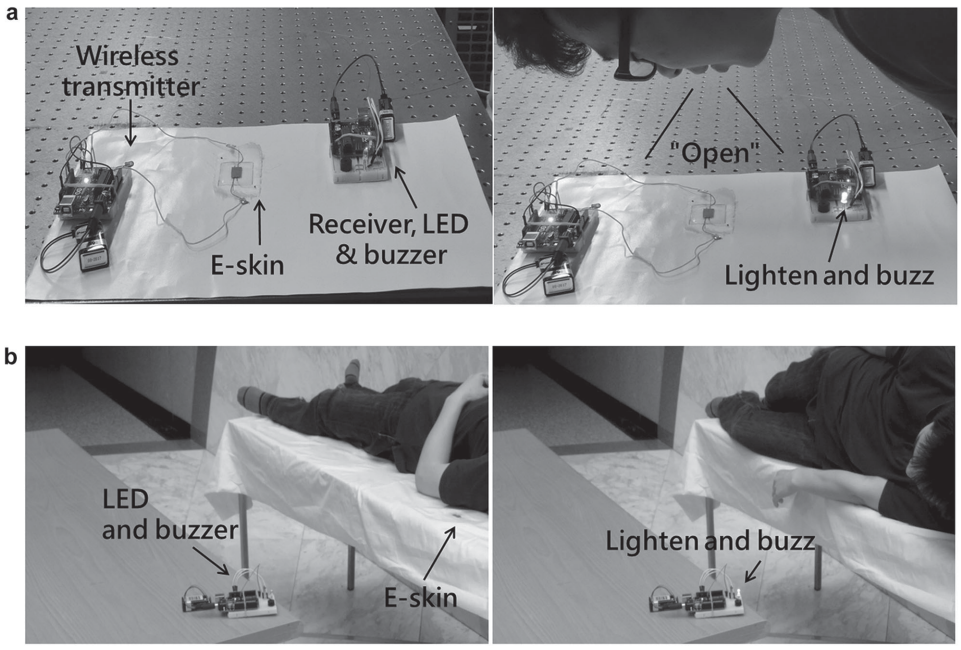

Figure 5. a) Photographs of the wireless sound controller system by using an as-prepared e-skin device. b) Photographs of the wireless monitor for detecting human motion on bed.

transmitter on the circuit (i.e., wireless e-skin controller), and another unit with a wireless receiver was designed to control an LED and buzzer (i.e., wireless responsive system). Once our skin-like sensor perceives sensing signals, the transmitter will wirelessly forward signals to the receiver and respond with turning on the LED and creating buzzing (Multimedia 4, Supporting Information). Based on the excellent sensitivity, the e-skin wireless controller can directly detect exhalation from human speaking and forward the signals. As demonstrated in Figure 5a(right), when the e-skin senses the exhalation from human speaking "open," the controller can wirelessly transmit "turn-on" signals to the receiver to light up the LED and buzz. From the demonstration, we can predict a variety of potential applications, such as wearable wireless human-interactive interfaces in smart systems that can be controlled by sound, muscle motions, gesture, or simply touch. In Figure 5b(left), we fabricated our e-skin device onto a bedspread by following the identical fabricating method and connected it with the wireless microcontroller systems the same as described above. In this design, we applied the device to wirelessly monitor human motion on a bed. When human moves to the edge of bed and triggers the e-skin, the transmitter will wirelessly send signals to the receiver to warn the danger of falling from the bed by buzzing and lighting up the LED (Figure 5b(right) and Multimedia 5, Supporting Information). This result shows that our methodology is suitable for different cloth-based articles and suggests its potential applications in assessing sleep quality, caring for the elderly, and monitoring patient motion on medical beds.

3. Discussion

Compared with previous methods,[11–20] including micro-pyramid-structured[14–16] or hollow-structured conducting materials[13] and metal-coated conducting tissue,[18] our method by self-bulged AgNW/PDMS can effectively suspend and lift the conducting materials, making the initial OFF-state at a break insulating condition. And, the highly conducting of AgNW film can make the ON-state current high enough for further integration with other functional devices, which renders to further explore more promising applications of electronic-skin/human-interactive devices, and the rough surface of stainless-steel threads and AgNW network leads to an unprecedented sensitivity, which is favorable for various fields where skin-like sensing is desired. Furthermore, our newly-designed cloth-based e-skin sensing device possesses numerous remarkable features and advantageous traits. First, the fabrication of the device based on a cloth substrate and conductive threads, rendering it good flexibility, stretchability, wearability, and feasibility to incorporate into textile-based articles, such as garment, wristbands, beds, and so forth. Second, by bridging highly conducting AgNW films from the initial open circuit, our device possesses ultrahigh current-switching ratios of $\approx 10^7$ orders of magnitude in response to the applied pressures in low-pressure region (<1 kPa). This advantage endows our device to manifest sensing signals, promoting the usage of novel ultrasensitive e-skin integration with microcontroller or embedded systems as wearable smart interfaces for versatile applications, such as sound, gesture, or IOT (Internet of Things) controllers, which can be commanded directly through the sensing. Third, the unprecedented sensitivity in the low-pressure region makes our e-skin a good candidate in various kinds of applications where wearable and flexible skin-like tactile sensing is desired. Taking these features, for the first time, the e-skin device can not only act as ultrasensitive sensor but also be able to facilely integrate with various electronic elements as multifunctional usages manipulated directly by harnessing the sensing capability. And, notably,

these remarkable features were realized by an operating voltage as low as 0.1 V, allowing our e-skin can be easily powered by a portable and green power source, and in turn as a self-powered e-skin system. Finally, we stress here that the variety of demonstrations as well as the real-time measurements described above was derived from several different devices. These results therefore ensure that our newly-designed device can not only serve as a membrane switch, but also behave an excellent pressure sensor even for pressures below 1 kPa.

4. Conclusion

In summary, we have developed a new type of flexible resistive e-skin device based on a cloth substrate, conductive threads, and highly conducting AgNW films with a simple and cost-effective method. The device is initially at a break state, and pressure-induced suspended AgNW films bridging two conductive threads render a contact-resistive-type sensing device. This new device possesses unprecedented features including ultrahigh current-switching behavior of $\approx 10^7$ and extremely-high sensitivity of 1.04×10^4–6.57×10^6 kPa^{-1} at pressures <3 kPa. To our knowledge, these are the highest values ever reported. In particular, they were achieved by a very low operating voltage of 0.1 V. The capability of perceiving various mechanical forces, throat muscle motions, and hand motions has been demonstrated. These exceptional features endow our ultrasensitive e-skin with remarkable capabilities of facile integration with other functional devices for diverse applications. We have successfully demonstrated the first example of fully autonomous indoor-light-powered e-skin system as information transmission. Furthermore, pressure-visible user-interactive e-skins with low detection limitation, ultrahigh sensitivities, and low driving voltage were first realized at pressures <1 kPa. Finally, a wireless sound controller and monitor were illustrated for sophisticated uses interacted through the sensing signals. We believe that our new methodologies presented here will open up a new perspective of ultrasensitive e-skins and will be largely beneficial in vast fields ranging from conformable sensors, indoor-light-powered robotic skins, fully autonomous health/medical monitors, to wearable smart interfaces.

Supporting Information

Supporting Information is available from the Wiley Online Library or from the author.

Acknowledgements

This work was supported by grants from the National Science Council and Ministry of Education of the Republic of China. The authors thank Prof. Chung-Chih Wu, Wei-Lung Tsai, and Chun-Yang Lu for assistance with OLED measurement. Y.C.L. would like to thank Chang-Chen Tsao for his suggestion in materials processing.

Received: August 26, 2015
Revised: November 15, 2015
Published online: January 12, 2016

[1] T. Someya, T. Sekitani, S. Iba, Y. Kato, H. Kawaguchi, T. Sakurai, *Proc. Natl. Acad. Sci. USA* **2004**, *101*, 9966.
[2] D.-H. Kim, N. Lu, R. Ma, Y.-S. Kim, R.-H. Kim, S. Wang, J. Wu, S. M. Won, H. Tao, A. Islam, *Science* **2011**, *333*, 838.
[3] S. C. Mannsfeld, B. C. Tee, R. M. Stoltenberg, C. V. H. Chen, S. Barman, B. V. Muir, A. N. Sokolov, C. Reese, Z. Bao, *Nat. Mater.* **2010**, *9*, 859.
[4] S. Bauer, *Nat. Mater.* **2013**, *12*, 871.
[5] M. L. Hammock, A. Chortos, B. C. K. Tee, J. B. H. Tok, Z. Bao, *Adv. Mater.* **2013**, *25*, 5997.
[6] S. Bauer, S. Bauer-Gogonea, I. Graz, M. Kaltenbrunner, C. Keplinger, R. Schwödiauer, *Adv. Mater.* **2014**, *26*, 149.
[7] B. C. Tee, C. Wang, R. Allen, Z. Bao, *Nat. Nanotechnol.* **2012**, *7*, 825.
[8] C. Wang, D. Hwang, Z. Yu, K. Takei, J. Park, T. Chen, B. Ma, A. Javey, *Nat. Mater.* **2013**, *12*, 899.
[9] J. Lee, H. Kwon, J. Seo, S. Shin, J. H. Koo, C. Pang, S. Son, J. H. Kim, Y. H. Jang, D. E. Kim, *Adv. Mater.* **2015**, *27*, 2433.
[10] B. C. K. Tee, A. Chortos, R. R. Dunn, G. Schwartz, E. Eason, Z. Bao, *Adv. Funct. Mater.* **2014**, *24*, 5427.
[11] H.-H Chou, A. Nguyen, A. Chortos, J. W. F. To, C. Lu, J. Mei, T. Kurosawa, W.-G. Bae, J. B.-H. Tok, Z. Bao, *Nat. Commun.* **2015**, *6*, 8011.
[12] Q. Sun, D. H. Kim, S. S. Park, N. Y. Lee, Y. Zhang, J. H. Lee, K. Cho, J. H. Cho, *Adv. Mater.* **2014**, *26*, 4735.
[13] L. Pan, A. Chortos, G. Yu, Y. Wang, S. Isaacson, R. Allen, Y. Shi, R. Dauskardt, Z. Bao, *Nat. Commun.* **2014**, *5*, 3002.
[14] B. Zhu, Z. Niu, H. Wang, W. R. Leow, H. Wang, Y. Li, L. Zheng, J. Wei, F. Huo, X. Chen, *Small* **2014**, *10*, 3625.
[15] X. Wang, Y. Gu, Z. Xiong, Z. Cui, T. Zhang, *Adv. Mater.* **2014**, *26*, 1336.
[16] C. L. Choong, M. B. Shim, B. S. Lee, S. Jeon, D. S. Ko, T. H. Kang, J. Bae, S. H. Lee, K. E. Byun, J. Im, *Adv. Mater.* **2014**, *26*, 3451.
[17] J. Park, Y. Lee, J. Hong, M. Ha, Y.-D. Jung, H. Lim, S. Y. Kim, H. Ko, *ACS Nano* **2014**, *8*, 4689.
[18] S. Gong, W. Schwalb, Y. Wang, Y. Chen, Y. Tang, J. Si, B. Shirinzadeh, W. Cheng, *Nat. Commun.* **2014**, *5*, 3132.
[19] G. Schwartz, B. C.-K. Tee, J. Mei, A. L. Appleton, D. H. Kim, H. Wang, Z. Bao, *Nat. Commun.* **2013**, *4*, 1859.
[20] Y. Zang, F. Zhang, D. Huang, X. Gao, C.-a. Di, D. Zhu, *Nat. Commun.* **2015**, *6*, 6269.
[21] W. Wu, X. Wen, Z. L. Wang, *Science* **2013**, *340*, 952.
[22] G. Zhu, W. Q. Yang, T. Zhang, Q. Jing, J. Chen, Y. S. Zhou, P. Bai, Z. L. Wang, *Nano Lett.* **2014**, *14*, 3208.
[23] S. Wang, L. Lin, Z. L. Wang, *Nano Energy* **2015**, *11*, 436.
[24] M. Kaltenbrunner, T. Sekitani, J. Reeder, T. Yokota, K. Kuribara, T. Tokuhara, M. Drack, R. Schwödiauer, I. Graz, S. Bauer-Gogonea, *Nature* **2013**, *499*, 458.
[25] W. Zeng, L. Shu, Q. Li, S. Chen, F. Wang, X. M. Tao, *Adv. Mater.* **2014**, *26*, 5310.
[26] W. Seung, M. K. Gupta, K. Y. Lee, K.-S. Shin, J.-H. Lee, T. Y. Kim, S. Kim, J. Lin, J. H. Kim, S.-W. Kim, *ACS Nano* **2015**, *9*, 3501.
[27] J. Zhong, Y. Zhang, Q. Zhong, Q. Hu, B. Hu, Z. L. Wang, J. Zhou, *ACS Nano* **2014**, *8*, 6273.
[28] D. Langley, G. Giusti, C. Mayousse, C. Celle, D. Bellet, J.-P. Simonato, *Nanotechnology* **2013**, *24*, 452001.
[29] J. P. Lynch, K. J. Loh, *Shock Vib. Dig.* **2006**, *38*, 91.
[30] L. Mottola, G. P. Picco, *ACM Comput. Surv. (CSUR)* **2011**, *43*, 19.
[31] L. Atzori, A. Iera, G. Morabito, *Comput. Netw.* **2010**, *54*, 2787.
[32] M. B. Schubert, J. H. Werner, *Mater. Today* **2006**, *9*, 42.
[33] S. Niu, Z. L. Wang, *Nano Energy* **2014**, *14*, 161.
[34] D. Son, J. Lee, S. Qiao, R. Ghaffari, J. Kim, J. E. Lee, C. Song, S. J. Kim, D. J. Lee, S. W. Jun, *Nat. Nanotechnol.* **2014**, *9*, 397.